Citation
Li, Z. and Chen, W. and Hao, H. and Khan, M.Z.N. 2021. Physical and Mechanical Properties of New Lightweight Ambient-Cured EPS Geopolymer Composites. Journal of Materials in Civil Engineering. 33 (6): ARTN 04021094. http://doi.org/10.1061/(ASCE)MT.1943-5533.0003705

Physical and mechanical properties of new lightweight ambient-cured EPS geopolymer composites

Zhixing Li[1]; Wensu Chen, M. ASCE[2]; Hong Hao, F. ASCE[3]; Musaad Zaheer Nazir Khan[4]

Abstract: Lightweight concrete (LWC) has been developed and used in both structural and non-structural applications. With an increasing demand for sustainable construction materials, geopolymer as an eco-friendly material has been intensively investigated. This study developed a newly synthesized lightweight ambient-cured geopolymer composite (LGC) by replacing natural fine aggregate with expanded polystyrene (EPS) beads at 10%, 20% and 30% in volume for various structural or non-structural purposes. The obtained composite was characterized with regard to its physical and mechanical properties. The interfacial area between the geopolymer matrix and EPS beads were observed. The properties of the developed LGC at fresh and hardened states, such as density, workability, compressive and splitting tensile strength, modulus of elasticity and Poisson's ratio were obtained and compared. The test results showed that the EPS inclusion had a significant effect on the properties of LGC. Besides, empirical formulae for predicting the compressive strength, modulus of elasticity and splitting tensile strength of the developed LGC were proposed.

[1]PhD student, Centre for Infrastructural Monitoring and Protection, School of Civil and Mechanical Engineering, Curtin University, Perth 6102, Australia. Email: zhixing.li@postgrad.curtin.edu.au

[2]Senior Lecturer, Centre for Infrastructural Monitoring and Protection, School of Civil and Mechanical Engineering, Curtin University, Perth 6102, Australia (corresponding author). Email: wensu.chen@curtin.edu.au

[3]John Curtin Distinguished Professor, Centre for Infrastructural Monitoring and Protection, School of Civil and Mechanical Engineering, Curtin University, Perth 6102, Australia (corresponding author). Email: hong.hao@curtin.edu.au

[4]Assistant Professor, NUST Institute of Civil Engineering, School of Civil and Environmental Engineering, National University of Sciences and Technology, Sector H-12, Islamabad, Pakistan. Email: musaad@nice.nust.edu.pk

Author Keywords: Expanded polystyrene; Lightweight geopolymer composite; Ambient-cured; Physical properties; Mechanical properties

Introduction

Lightweight concrete (LWC) has been produced for various construction applications, such as load-bearing hollow bricks and blocks, cladding panels, slabs, and reinforced concrete beams (Cook 1983; Tang et al. 2006; Xu et al. 2012; Demirel 2013). There are several characteristics of LWC to satisfy the requirements of density and performance for various applications (Bogas et al. 2015; Aslam et al. 2016). Previous studies have indicated that for the structural purpose, the minimum compressive strength of LWC should be 17 MPa with a density of 1120~1920 kg/m^3 (ACI 2014). LWC with the compressive strength of 7~17 MPa and the density lower than 1840 kg/m^3 is known as moderate LWC (Topçu 1997; Glenn et al. 1998). The compressive strength of LWC for the insulation purpose ranges from 0.7 MPa to 7 MPa, and the density is expected to be either 800 kg/m^3 or lower (Sadrmomtazi et al. 2012). Depending on the requirements for various construction applications, lightweight aggregates could be incorporated in LWC by partially or totally replacing natural aggregate.

Expanded polystyrene (EPS) is an ultra-lightweight cellular plastic material with a density of 10~30 kg/m^3, which is widely used in decorative mouldings, lightweight packaging, energy absorption and insulation applications (Ravindrarajah and Tuck 1994; Doroudiani and Omidian 2010; Yoo and Qiu 2018). Currently, landfill and incineration are traditional disposal methods that lead to significant environmental issues. Even though several reuse processes have been developed for EPS, hazardous solvents are required to be used in most of the processes (Shin 2006; Amianti and Botaro

2008). Waste EPS is attracting attention as a common environmental issue, which can be recycled and used as lightweight aggregate for construction. Some of the previous studies have endeavoured to incorporate EPS in ordinary Portland cement (OPC) matrix (Babu and Babu 2003; Miled et al. 2007; Tang et al. 2008; Xu et al. 2012; Ferrándiz-Mas and García-Alcocel 2013; Tang et al. 2014). It has been reported that the replacement of natural aggregate by EPS would reduce the strength of LWC and the additional agents were required to enhance the mechanical performance of LWC. Besides, it has also been observed that using EPS can reduce the restraint effect and result in the increase of shrinkage and creep deformation, owing to the lower static modulus of elasticity (Hansen and Nielsen 1965; Hobbs 1969; Hobbs 1974; Leemann et al. 2011). Other studies evaluated the effect of the size distribution of EPS and mix proportions on the properties of LWC (Miled et al. 2007; Falzone et al. 2016).

In addition, OPC as the binder of conventional concrete is the most widely used construction material (Benhelal et al. 2013). Limestone and fossil fuel as non-renewable natural resources are used for the production of OPC. CO_2 generated during the OPC manufacturing process is responsible for 5~7% of the total emissions, which gives a massive contribution to global warming (Huntzinger and Eatmon 2009; Pelisser et al. 2012). For sustainable development, it is essential to develop an alternative to OPC.

In the last two decades, geopolymer as an environment-friendly cementitious material has received significant interest. Unlike the OPC, the production of geopolymer involves the re-use of industrial by-products or wastes, such as metakaolin, fly ash, and blast furnace slag, etc. (Chuah et al. 2016; Tang et al. 2020). Geopolymer has displayed the potential to diminish relevant greenhouse gas emissions up to 80% with reasonable strengths and great physical properties, i.e. low water

permeability, efficient thermal stability, and low shrinkage (Provis and Van Deventer 2009; Atiş et al. 2015; Nasvi et al. 2016; Hu et al. 2019). It is believed that geopolymer concrete as a green material can be potentially used in multiple applications such as structural, fire-resistant, and thermal insulating purposes. Recently, a newly synthesized ambient-cured geopolymer was developed using slag as part of the binder (Nath and Sarker 2014; Khan et al. 2016; Tao and Pan 2019). In contrast to the heat curing, the ambient-cured geopolymer is more feasible for onsite construction.

Lightweight geopolymer composite (LGC) as a novel lightweight material is developed by replacing OPC with geopolymer as the matrix. Currently, there are very limited studies on the properties of LGC made by substituting natural aggregates with EPS. Most of them focused on the thermal and mechanical properties of heated-cured LGC containing EPS (Posi et al. 2015; Singh et al. 2015; Colangelo et al. 2018; Kakali et al. 2018). Besides, bonding additives or admixtures, i.e. epoxy resin, styrene-butadiene-styrene latex, and lightweight agents, etc., were required to avoid the segregation phenomenon of EPS in the heat-cured matrix. It was reported that the replacement of natural aggregate by EPS significantly improved the thermal insulation and reduced the strength of LGC. Aslani et al. (2020) developed ambient-cured LGC with chemical treated polystyrene which used viscosity modifying agent as an admixture and indicated that the LGC with a density ranging from 1750 to 2200 kg/m^3 could be obtained having a compressive strength of 7.70~25.40 MPa. However, the studies on ambient-cured LGC with lower density ranges are still lacking. In the present study, ambient-cured LGC using untreated EPS beads as lightweight aggregate was established without the addition of bonding additives or admixtures, which highlights the uniqueness of the developed LGC. The targeted compressive strength and the density of LGC varied from 6.32 to 24.33 MPa and 1284.31 to 1791.86 kg/m^3, respectively.

In this study, plain geopolymer mortar (GM) and LGC containing EPS beads with volume fractions of 10%, 20% and 30% were prepared. The microstructural analysis characterized the interfacial transition zones (ITZ) between the geopolymer matrix and EPS beads by scanning electron microscopy (SEM) analysis. The physical properties of plain GM and LGC including density, workability, ultrasonic pulse velocity (UPV), and X-ray diffraction (XRD) patterns were investigated. The compressive and splitting tensile strength, modulus of elasticity and Poisson's ratio of plain GM and LGC with different EPS content were obtained. The experimental results were compared with the existing models from the previous studies, followed by proposing empirical formulae to predict the compressive strength, modulus of elasticity and splitting tensile strength of the developed LGC.

Experimental program

Material

The fly ash (FA) (specific gravity = 2.35) with class F as per ASTM C618-19 (ASTM 2019) was supplied by Cement Australia from the Gladstone power station in Queensland, Australia. The commercially available slag with a specific gravity of 2.80 was provided by BGC cement Australia. The EPS beads with a density of 20.13 kg/m^3 and a diameter of 5 mm were used as lightweight aggregate. The 8 M sodium hydroxide (NaOH) solution (molarity = 8 mol/L) was prepared at least 24 hours before casting by dissolving 97-98% pure NaOH solid into the tap water. The D-grade sodium silicate (Na_2SiO_3) solution with a specific gravity of 1.53 was obtained from PQ Australia Ltd. Silica sand with a fineness modulus of 2.77 and a specific gravity of 2.65 was supplied by Hanson Construction Materials. The constituents of raw ingredients were obtained via X-ray fluorescence

analysis. The chemical compositions of FA, slag, and sodium silicate (Na_2SiO_3) are provided in Table 1.

Table 1. Chemical compositions (weight %) of fly ash, slag, and sodium silicate (Na_2SiO_3).

Composition (wt.%)	Fly ash	Slag	Sodium silicate
SiO_2	51.1	32.5	29.4
Na_2O	0.77	0.27	14.7
H_2O	-	-	55.9
Al_2O_3	25.56	13.56	-
Fe_2O_3	12.48	0.85	-
CaO	4.3	41.2	-
MgO	1.45	5.10	-
TiO_2	1.32	0.49	-
MnO	0.15	0.25	-
P_2O_5	0.885	0.03	-
K_2O	0.7	0.35	-
SO_3	0.25	3.2	-
Others	0.46	1.12	-
LOI	0.57	1.11	-

Note: LOI= Loss on ignition

Mix proportions, mixing, and curing of specimens

The mix proportioning of the plain GM and LGC was determined according to the previous study (Khan et al. 2016) to obtain the optimum mechanical properties. In the present study, the ratio of activator to binder in weight was determined as 0.40 for all mixtures. The fine aggregate/binder ratio in weight was determined as 1.60 for plain GM. 8M sodium hydroxide (NaOH) and D-grade sodium silicate solution (Na_2SiO_3) with a NaOH/Na_2SiO_3 ratio of 2.50 were used to prepare the alkaline activator. The use of slag can increase the viscosity of the geopolymer matrix, which results in the

reduction of the flow rate of the geopolymer matrix (Nath and Sarker 2014). Therefore, the FA to slag ratio was determined as around 5.60 to obtain the reasonable workability and preclude the segregation phenomenon of EPS beads. The details of the mix proportions are listed in Table 2.

Table 2. Mix proportions of plain geopolymer mortar (GM) and LGC.

Mix ID	Constituent mix proportions (kg/m^3)					EPS	
	FA	Slag	NaOH	Na_2SiO_3	Sand	Wt. (kg/m^3)	Vol (%)
Plain GM	595	105	80	200	1120	-	-
EPS-10	595	105	80	200	855	1.35	10%
EPS-20	595	105	80	200	590	2.70	20%
EPS-30	595	105	80	200	325	4.05	30%

The mixtures were prepared in a 70 L planetary mixer. Firstly, the activating solution was prepared for more than one hour before casting. The raw constituents including FA and slag were mixed with silica sand for 3 mins. Next, the mixture was allowed to homogenize for another 3 mins after pouring the alkaline activator into the mixer slowly. Then, EPS beads were distributed into geopolymer mortar. After that, EPS beads and geopolymer mortar were panned mixed. The flow tests were conducted shortly after mixing. Subsequently, mixtures were cast into cylindrical moulds (Ø100 × 200 mm and Ø150 × 300 mm) in three layers with 30s slight vibration. The sealed specimens were cured at the ambient condition for 24 hours. After demoulding, the wrapped specimens were cured with a pre-set temperature of 22 ± 2℃ and relative humidity of 50 ± 5% for 28 days. The chosen curing condition was according to the standard by the International Organization for Standardization (Feng et al. 2014). The uniform distributions of EPS beads along the cross-section of specimens with different EPS content are shown in Fig. 1.

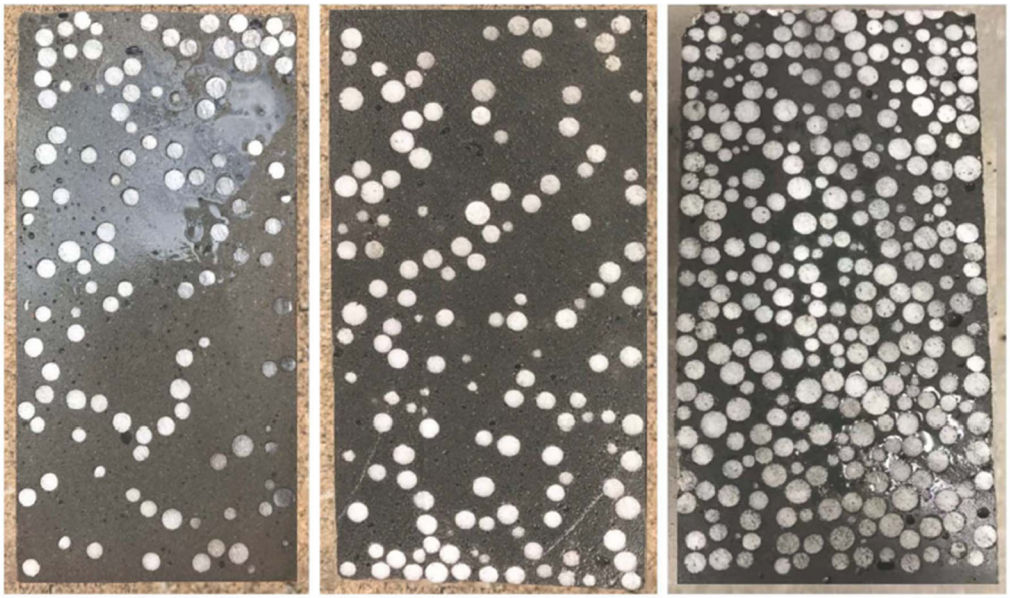

Fig. 1. Distribution of EPS beads along cross-section of specimens (a) EPS-10; (b) EPS-20; (c) EPS-30.

Experimental methodology

Density and workability

The density of the freshly mixed composites was evaluated as per ASTM C1688-14 (ASTM 2014). The average value of three specimens for each configuration was calculated for the analysis. The workability of the mixture was evaluated according to the flow rate test based on the guidelines stipulated in ASTM C1437-15 (ASTM 2015). At least two replicates were tested for each casting with different EPS content.

Quasi-static tests

Quasi-static compressive and splitting tensile tests were conducted by using a SHIMADZU testing machine with the capability of loads up to 300 kN. The test setups are shown in Fig. 2. For the quasi-static compressive test, at least three sulphur capped cylindrical specimens with Ø100 × 200 mm were tested with an equivalent loading rate of 0.33 MPa/min in accordance with ASTM C39-

18 (ASTM 2018). As shown in Fig. 2 (a), the longitudinal strain of the specimen was measured by using the 50-mm length strain gauge with a sensitivity factor of 2.0 and a resistance of 120 Ω. A pair of strain gauges were attached longitudinally on opposite sides of the specimen at mid-height. The obtained values of strain data were used to present the stress-strain behaviour for plain GM and LGC specimens.

For the quasi-static splitting tensile test, at least three cylindrical specimens of Ø150 × 300 mm for each configuration were tested under a loading rate of 0.70 MPa/min as per ASTM C496-17 (ASTM 2017). Fig. 2 (b) shows the compressive platens were used to sandwich the specimen horizontally. To preclude the compressive stress concentration around the point of loading, two pieces of wood were placed between the compressive platens and the test specimen to ensure uniform stress distribution.

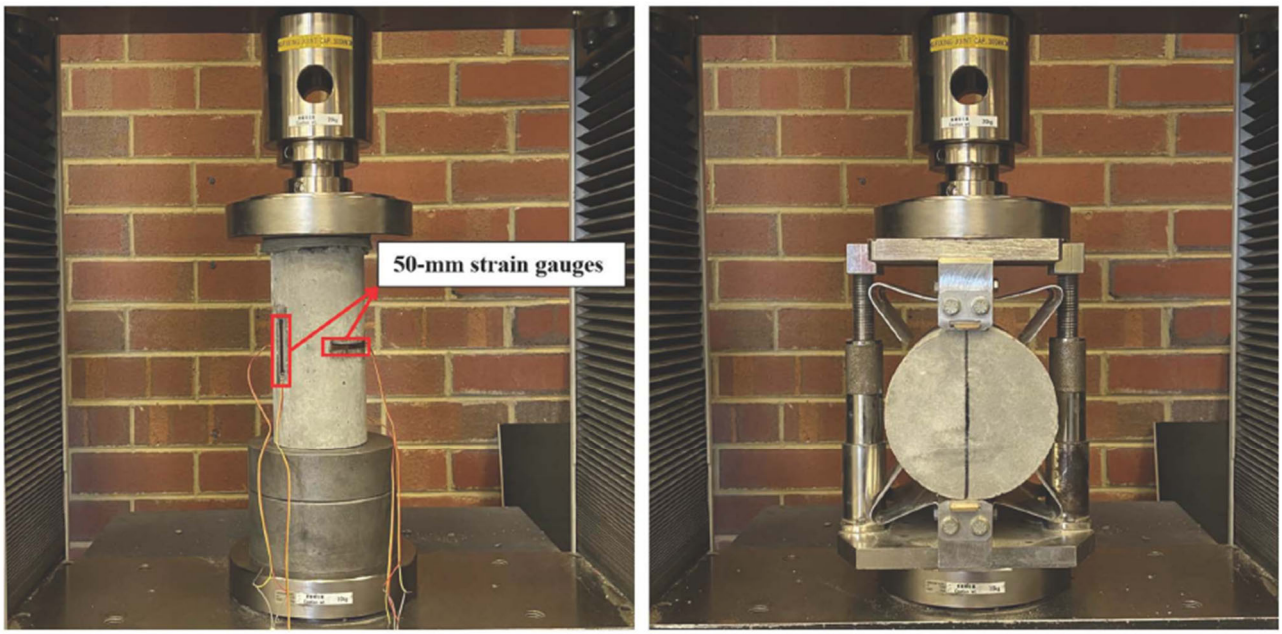

Fig. 2. Test setups for (a) compressive test; (b) splitting tensile test.

Modulus of elasticity and Poisson's ratio

Modulus of elasticity (E) and Poisson's ratio (μ) were determined based on the guidelines given in ASTM C469-14 (ASTM 2014). As shown in Fig. 2 (a), the longitudinal strains were obtained from two strain gauges with a length of 50 mm. The transverse strain was measured by a pair of 50 mm-length strain gauges attached perpendicularly to the direction of compression in the middle of the specimen. At least three specimens were tested for each configuration and the average value was calculated for the analysis. The modulus of elasticity (E) and Poisson's ratio (μ) can be calculated as follows:

$$E = (S_2 - S_1) / (\varepsilon_2 - \varepsilon_1) \quad (1)$$

where S_2 = stress corresponding to 40 % of ultimate load; ε_1 = longitudinal strain of 0.000050, MP; S_1 = stress corresponding to the longitudinal strain ε_1; ε_2 = longitudinal strain corresponding to stress S_2.

$$\mu = (\varepsilon_{t2} - \varepsilon_{t1}) / (\varepsilon_2 - \varepsilon_1) \quad (2)$$

where ε_{t2} = transverse strain at mid-height of the specimen corresponding to stress S_2; ε_{t1} = transverse strain at mid-height of the specimen corresponding to stress S_1.

Ultrasonic pulse velocity (UPV) test

The quality and strength of plain GM and LGC were evaluated by the UPV test as per ASTM C597-16 (ASTM 2016). During the tests, the compressive waves were generated by transducers having a diameter of 25 mm and a central frequency of 200 kHz. The propagation time of the ultrasonic wave through the 100 × 200 mm cylindrical specimens was measured. At least two specimens for each configuration were tested. The test set-up of the UPV test is presented in Fig. 3.

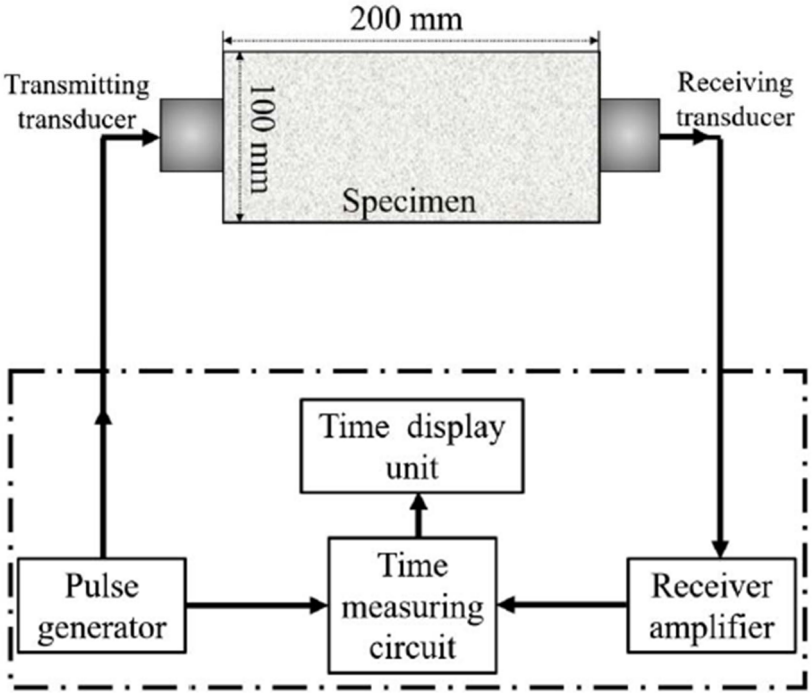

Fig. 3. The test set-up of ultrasonic pulse velocity test.

X-ray diffraction (XRD) analysis

The crystalline information of raw ingredients, plain GM, and LGC was determined by XRD analysis. EPS-20 was tested as a representative sample of LGC. Randomly oriented powder samples from the tested specimens were prepared in the disc container and the XRD patterns were determined by the Bruker-AXS D8 Advance Diffractograms. The factor of the diffractograms scanning was 2-theta values between 10° and 90° at a step size of 0.02°. The phase identification for the samples was carried out in DIFFRAC.EVA program.

Scanning electron microscopy (SEM) analysis

Microstructural analyses were conducted via SEM as per ASTM C1723-16 (ASTM 2016). The cubic specimens with dimensions of 10 mm were cut from the representative cylinder specimens.

SEM images were obtained from a Zeiss EVO 40XVP microscope on freshly prepared fractured surfaces.

Results and discussions

Density and workability

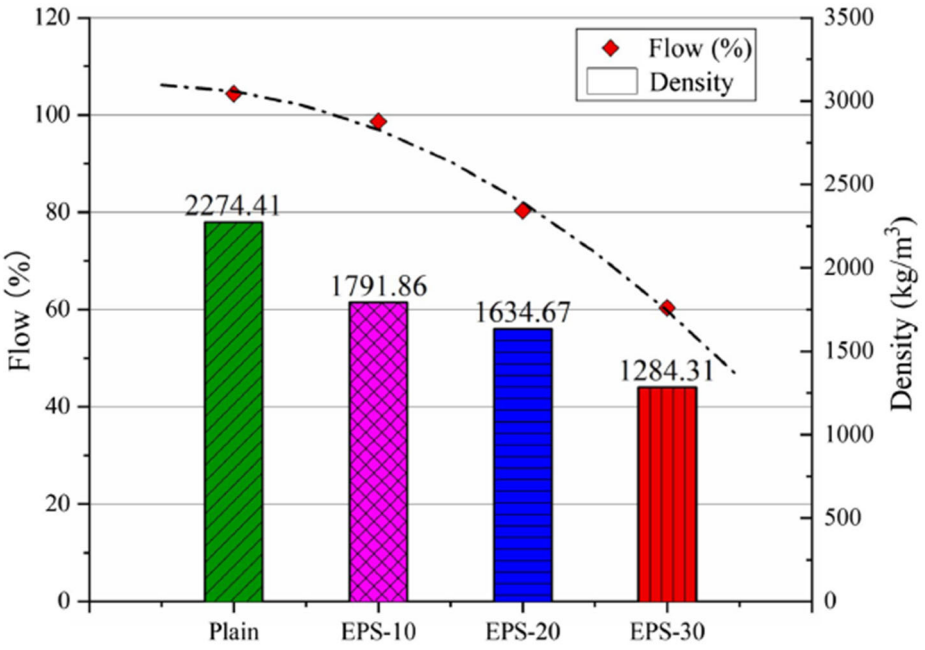

Fig. 4. Effect of EPS contents on density and workability of plain GM and LGC.

The fresh properties of plain GM and LGC including the density and flow rates are presented in Fig. 4. The workability of plain GM and LGC was evaluated by the flow rate test. As shown, with the increase of EPS volume fractions, the density and workability are reduced. The flow rate of plain GM with a density of 2274.41 kg/m^3 is 104.33%. The densities of LGC with the replacement of EPS by 10%, 20% and 30% in volume decrease to 1791.86 kg/m^3, 1634.67 kg/m^3, and 1284.31 kg/m^3, respectively. In this study, the densities of developed LGC are within the range of lightweight concrete as specified in (Cook 1983). Besides, the reductions in flow rates of the LGC with replacement EPS by 10%, 20% and 30% in volume are 5.47%, 23.07% and 42.31%, respectively, as

compared with plain GM. This is mainly because EPS has ultra-lightweight and hydrophobic nature as compared with the natural aggregates, which can reduce the weight of LGC to flow under gravity. Similar observations were reported by Aslani et al. (2020) on LGC.

Quasi-static compressive strength

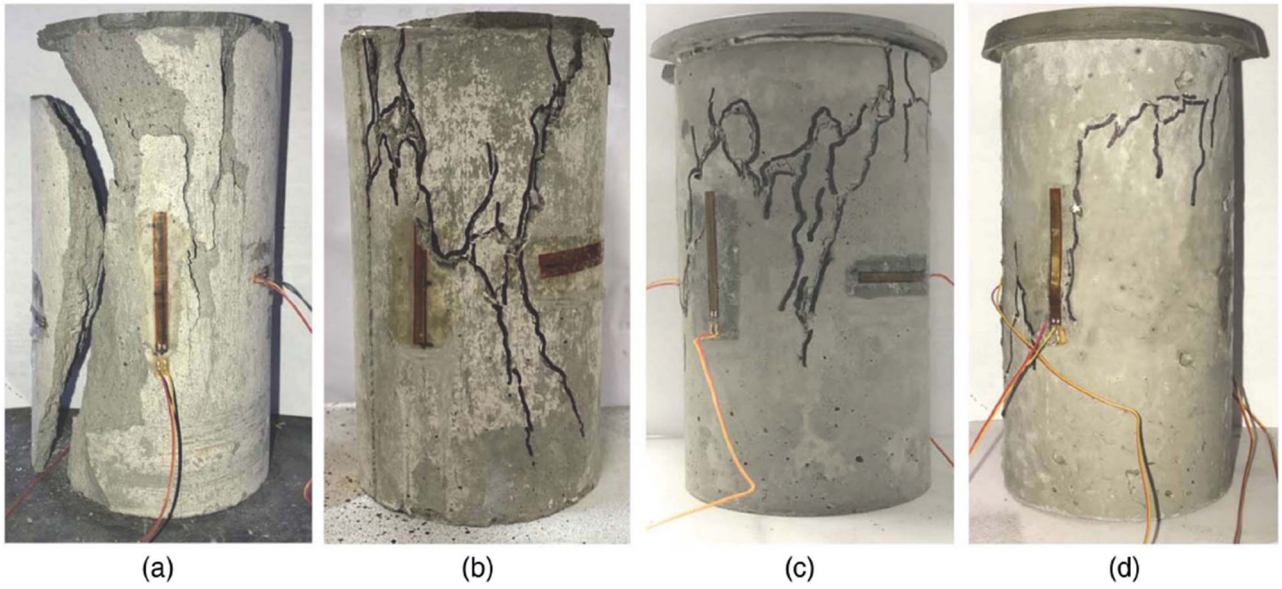

Fig. 5. Failure modes of specimens after compressive tests (a) Plain GM; (b) EPS-10; (c) EPS-20; (d) EPS-30.

Fig. 5 presents the typical failure modes of plain GM and LGC after the compressive test. It is observed that the specimen of plain GM failed into several chunks. The specimen containing 10% EPS (labelled as EPS-10) exhibits cracks over the whole specimens, whereas the specimen containing 30% EPS in volume (labelled as EPS-30) affects only one-third height from the top surface of the specimen. The failure modes of LGC change from global failure to local failure with the increase of EPS contents. Lateral bulging can be observed in the failure part of the specimens, which is consistent with the previous study (Babu et al. 2005). The local failure mode indicates that LGC with higher EPS contents behave like energy-absorbing and cushioning materials.

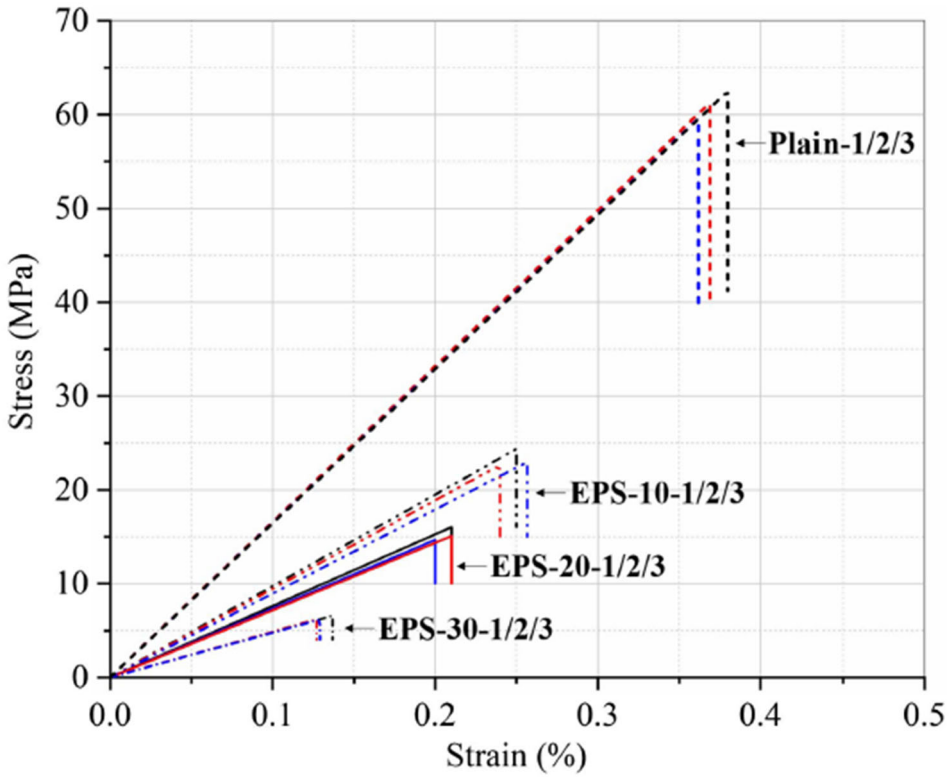

Fig. 6. Stress-strain behaviour of plain GM and LGC.

Fig. 6 shows the engineering stress-strain curves for all specimens of plain GM and LGC in compression. As shown, plain GM and LGC specimens experience linear stress-strain behaviours under compressive loading. All three tested specimens of plain GM fail with average ultimate stress of 61.12 MPa and an average failure strain of 0.36%. A sudden drop after reaching peak stress is mainly due to the brittle nature of the geopolymer composite. The similar stress-strain curves were observed in the previous studies (Pan and Sanjayan 2010; Khandelwal et al. 2013). The stress-strain curves of all nine LGC specimens are also shown in Fig. 6. It is shown that all curves have similar trends and the specimens experience brittle failure after reaching peak stress. In the present study, no bonding additives/admixtures and coarse aggregate have been used in LGC. Therefore, the stress-strain behaviour of LGC primarily relies on the properties of the geopolymer matrix. With an increase in the EPS contents, both failure strain and Young's modulus of LGC decrease, as expected. For instance, the average failure strains of LGC with the EPS volume fractions of 10%, 20% and 30% are

about 0.24%, 0.21% and 0.13%, respectively. The average failure strains of LGC with the EPS volume fractions of 10%, 20% and 30% are about 0.24%, 0.21% and 0.13%, respectively. It is noted that the compressive strain capacity of LGC with 10%, 20% and 30% EPS contents is reduced by around 33.33%, 41.66% and 63.89% as compared to that of plain GM, respectively, which indicates the increased brittleness of LGC with the increase of EPS contents.

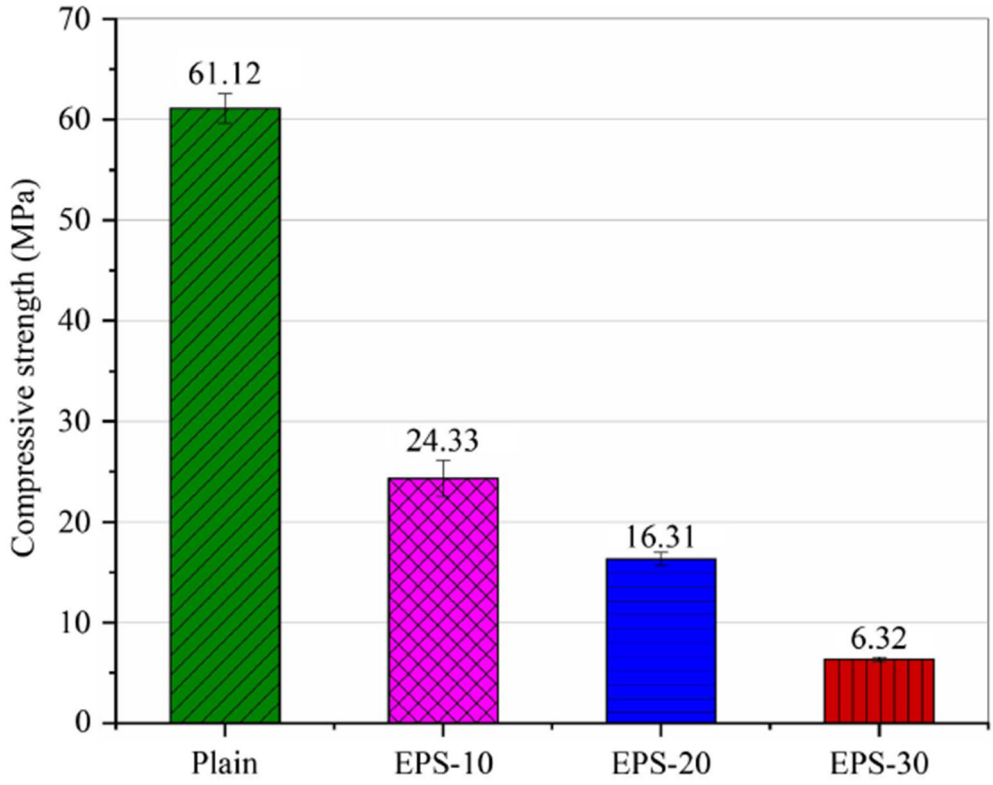

Fig. 7. Compressive strength of plain GM and LGC.

The results of quasi-static compressive tests for plain GM and LGC with different EPS volume fraction are shown in Fig. 7. The compressive strength of LGC decreases as the volume fractions of EPS increases. It is observed that the compressive strength of plain GM is 61.12 MPa. The replacement of EPS by 10%, 20% and 30% leads to the compressive strength of 24.33 MPa, 16.31 MPa and 6.32 MPa, respectively. As compared to plain GM, the reduction in the compressive strength of LGC with the replacement of 10% and 20% EPS is around 60% and 73%, respectively. It should

be noted that the compressive strength is reduced by 90% when 30% of natural fine aggregates volume is replaced by EPS. This can be due to the low strength of EPS and the weak bonding between EPS and matrix (Tamut et al. 2014; Tang et al. 2016). In this study, LGC with the replacement of EPS by 10% in volume (labelled as EPS-10) has the compressive strength 24.33 MPa and the density 1791.86 kg/m^3, which meets the requirement of structural lightweight concrete, i.e. compressive strength higher than 17 MPa and the density between 1120 and 1920 kg/m^3 as specified in ACI 213R-14 (ACI 2014). Besides, LGC with the replacement of EPS by 20% in volume (labelled as EPS-20) having the compressive strength of 16.31 MPa and the density of 1634.67 kg/m^3 shows the properties of moderate strength lightweight concrete, i.e. compressive strength ranging from 7 to 17 MPa and the density lower than 1840 kg/m^3 (Glenn et al. 1998).

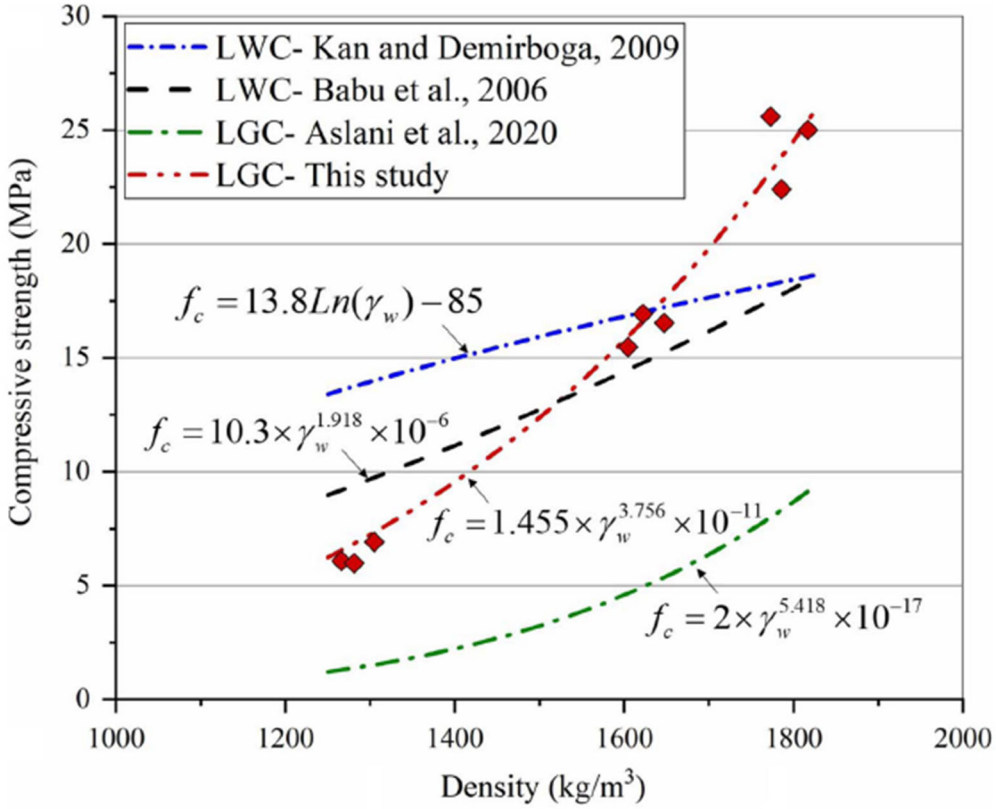

Fig. 8. Relationship between compressive strength and density.

Fig. 8 shows the relationship between the compressive strength and the density of LWC and LGC from the present study and previous studies. As shown, the compressive strength of developed LGC decreases with decreased density and increased EPS contents. Babu et al. (2006) compared their test results with previous studies and proposed an empirical model describing the relationship between the compressive strength and the density of LWC with EPS ranging from 200 to 2000 kg/m^3, expressed as:

$$f_c = 10.3 \times \gamma_w^{1.918} \times 10^{-6} \quad (3)$$

where f_c is the compressive strength (MPa), γ_w is the density (kg/m^3). Kan and Demirboğa (2009) proposed an empirical model for the LWC with the density varying from 980 to 2025 kg/m^3. The LWC was made of modified waste EPS with the density of 217 kg/m^3 and the diameter ranging from 4 to 16 mm, expressed as:

$$f_c = 13.8Ln(\gamma_w) - 85 \quad (4)$$

In a recent study, Aslani et al. (2020) also suggested an empirical model for ambient-cured LGC with the density ranging between 1750 and 2200 kg/m^3, which was made of chemical coated EPS with the density of 40 kg/m^3 and the diameter of 3 mm, expressed as:

$$f_c = 2 \times \gamma_w^{5.418} \times 10^{-17} \quad (5)$$

As shown in Fig. 8, the three empirical models for the above-mentioned LWC and LGC cannot well predict the compressive strength of the developed LGC in this study. The proposed empirical model (R^2= 0.956) for the relationship between the compressive strength and density of the developed LGC with density varying from 1284.31 to1791.86 kg/m^3 can be expressed as:

$$f_c = 1.455 \times \gamma_w^{3.756} \times 10^{-11} \quad (6)$$

In this study, the empirical model was proposed for the LGC made of 5 mm-diameter EPS beads with a density of 20.13 kg/m^3. It should be noted that various sizes and densities of EPS beads may result in different compressive strength and density of LGC. More experiments should be conducted in future studies to include different factors such as the size and density of EPS beads into the empirical formula.

Modulus of elasticity and Poisson's ratio

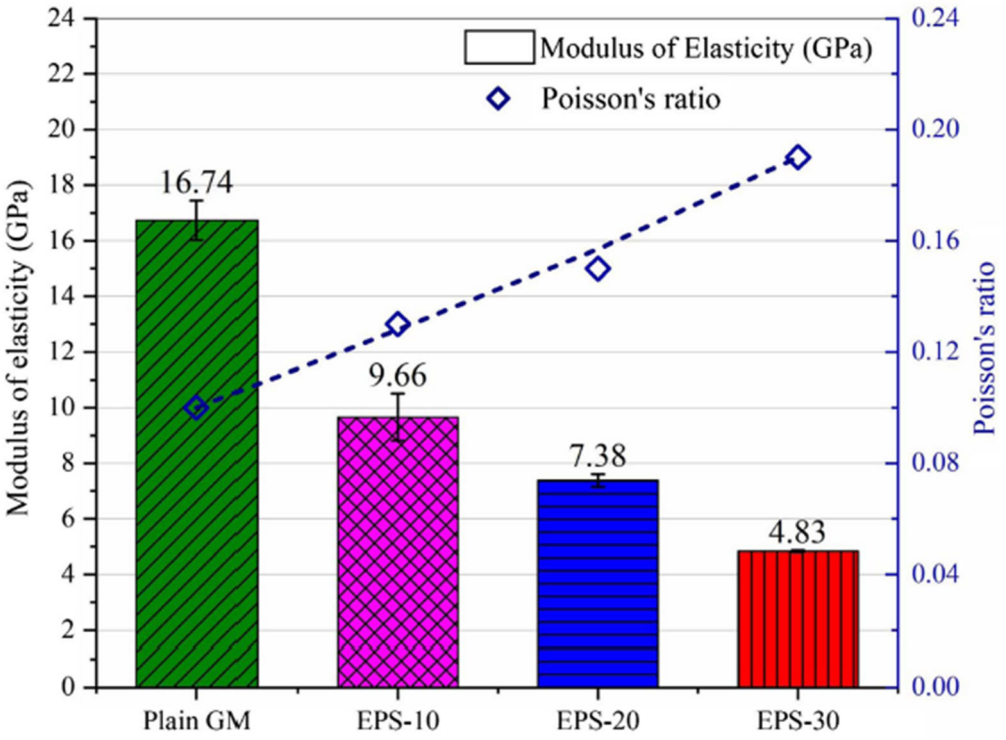

Fig. 9. Comparison of modulus of elasticity and Poisson's ratio of plain GM and LGC.

Fig. 9 shows the modulus of elasticity (E) and Poisson's ratio (μ) of plain GM and LGC. With the increase in EPS contents, the modulus of elasticity decreases while the Poisson's ratio increases. As observed, the mean value of the modulus of elasticity of plain GM is 16.74 GPa. By replacing 10% and 20% of natural fine aggregate volume by EPS beads, the modulus of elasticity decreases by 40% and 46%, respectively. It is noted that the modulus of elasticity for EPS-30 decreases by 70% as

compared with plain GM which is mainly attributed to the significantly lower modulus of elasticity of EPS than natural aggregates. As shown in **Fig. 9**, by replacing 10%, 20% and 30% of natural fine aggregate volume with EPS, the Poisson's ratio is enhanced to 0.13, 0.15 and 0.19, respectively, which is because of the higher deformability of EPS in contrast to the natural aggregate.

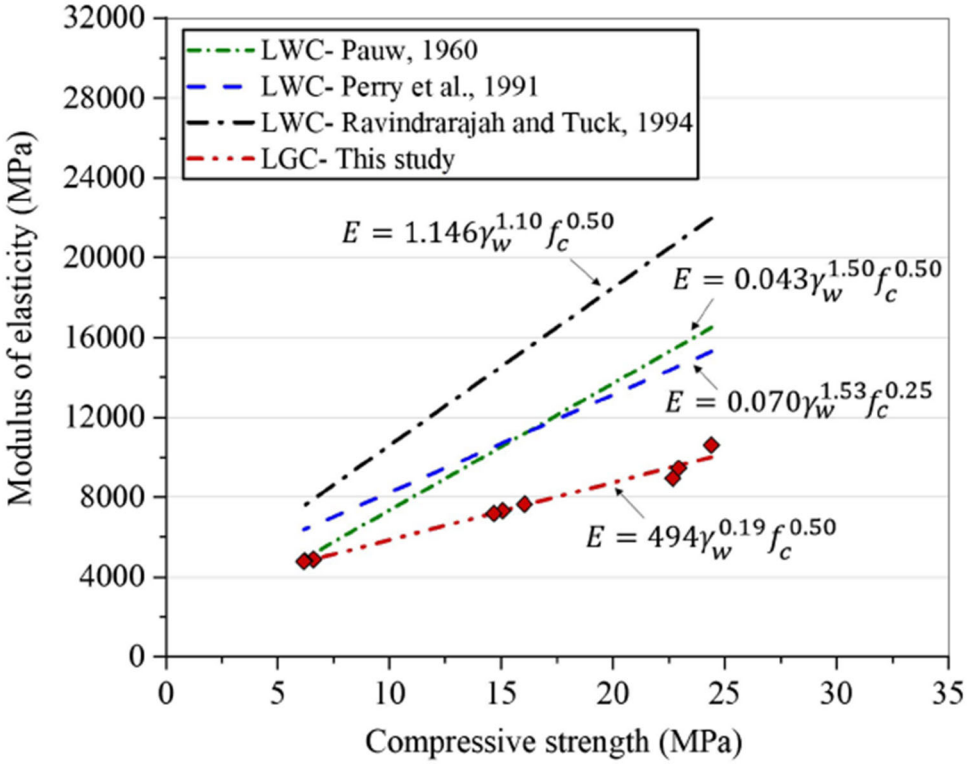

Fig. 10. Relationship between modulus of elasticity and compressive strength.

Fig. 10 shows the relationship between the modulus of elasticity and compressive strength of LWC and LGC from the present study and previous studies. It is found that the decrease in density can reduce the compressive strength, which leads to a decrease in the modulus of elasticity of LGC. This trend is similar to the results from the previous studies on LWC (Pauw 1960; Perry et al. 1991; Ravindrarajah and Tuck 1994). Pauw (1960) proposed an empirical model for the relationship between modulus of elasticity and compressive strength of LWC, expressed as:

$$E = 0.043\gamma_w^{1.50} f_c^{0.50} \quad (7)$$

where E is the modulus of elasticity (MPa), γ_W is dry density (kg/m^3), f_c is the mean compressive strength (MPa). Perry et al. (1991) and Ravindrarajah and Tuck (1994) proposed empirical formulae for the modulus of elasticity of LWC containing EPS, respectively, expressed as:

$$E = 0.070\gamma_w^{1.53} f_c^{0.25} \quad (8)$$

$$E = 1.146\gamma_w^{1.10} f_c^{0.50} \quad (9)$$

As shown in **Fig. 10**, the existing empirical models for predicting the modulus of elasticity of LWC are not applicable to the developed LGC in this study. The proposed empirical model of the developed LGC with density varying from 1284.31 to1791.86 kg/m^3 in the present study is given by:

$$E = 494\gamma_w^{0.19} f_c^{0.50} \quad (10)$$

The proposed formula for the developed LGC is similar to those empirical models for LWC even though the E value in this study is substantially lower than that of LWC in the previous studies. It is because the lack of coarse aggregates and the use of geopolymer mortar as a matrix can result in the decrease of elastic modulus (Pan et al. 2011). Besides, the density and sizes of the lightweight aggregate can also affect the modulus of elasticity. For example, the chemical coated 3 mm-diameter EPS was used as a lightweight aggregate, which can obtain a higher modulus of elasticity at the same compressive strength (Babu et al. 2005). As a result, various densities and sizes of EPS beads can be further considered to be included in the proposed model.

Quasi-static splitting tensile strength

The typical splitting failure modes of plain GM and LGC are shown in **Fig. 11**. It is observed that each specimen has a main central crack, satisfying the requirements for the splitting tensile test of concrete (ASTM 2017). The secondary crack is attributed to the propagation of micro-cracks

around EPS beads. During the splitting tensile test, the plain GM specimens split into two pieces at the peak loading, while the specimens experienced progressive failure as EPS contents increasing. The specimens EPS-30 did not exhibit an explosive failure.

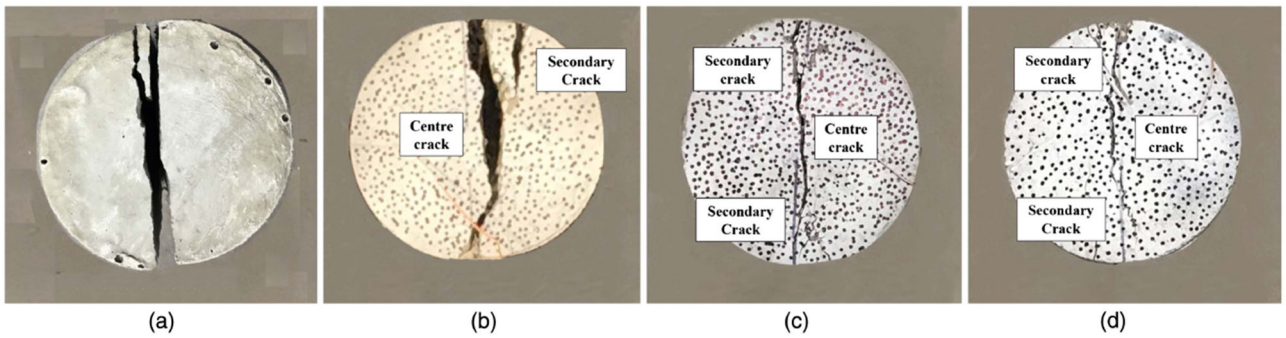

Fig. 11. Failure modes of specimens after splitting tensile test (a) Plain GM; (b) EPS-10; (c) EPS-20; (d) EPS-30.

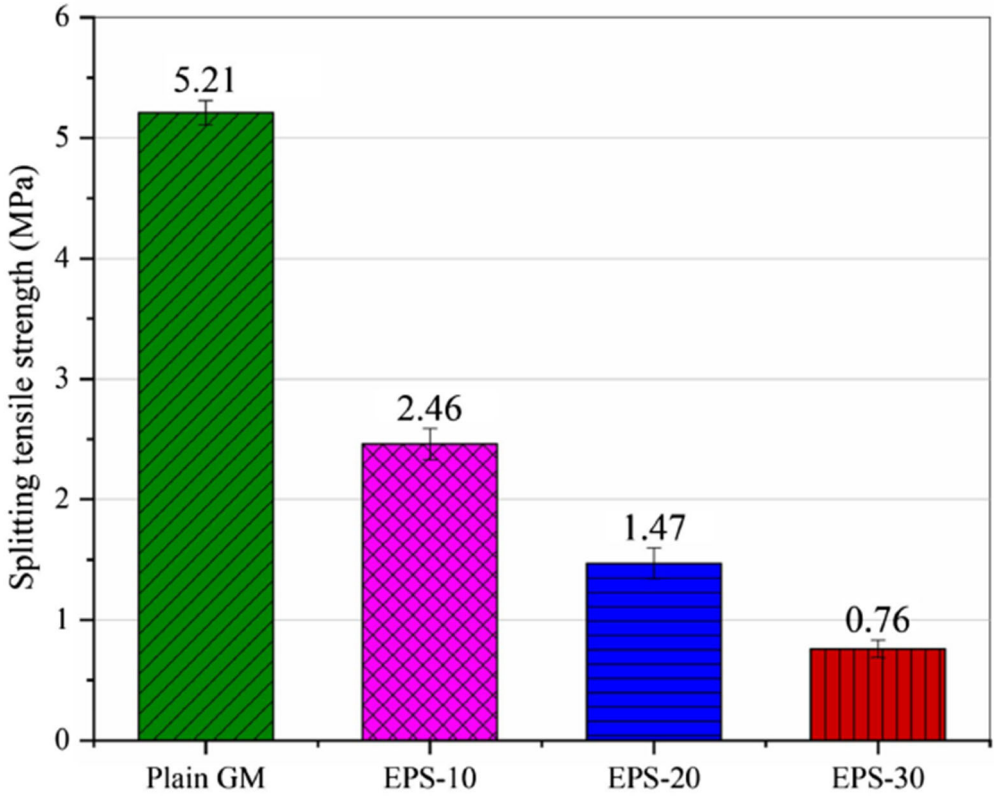

Fig. 12. Splitting tensile strength of plain GM and LGC.

The splitting tensile strength of plain GM and LGC with different EPS content are shown in **Fig. 12**. With the increase of EPS contents, the splitting tensile strength decreases. As shown, the splitting

tensile strength of plain GM is 5.21 MPa. By replacing 10%, 20% and 30% of natural fine aggregate volume with EPS, the splitting tensile strength decreases by 52.7%, 71.1% and 85.2%, respectively. It is mainly attributed to the decrease of the effective stress area with a higher volume fraction of EPS (Liu and Chen 2014).

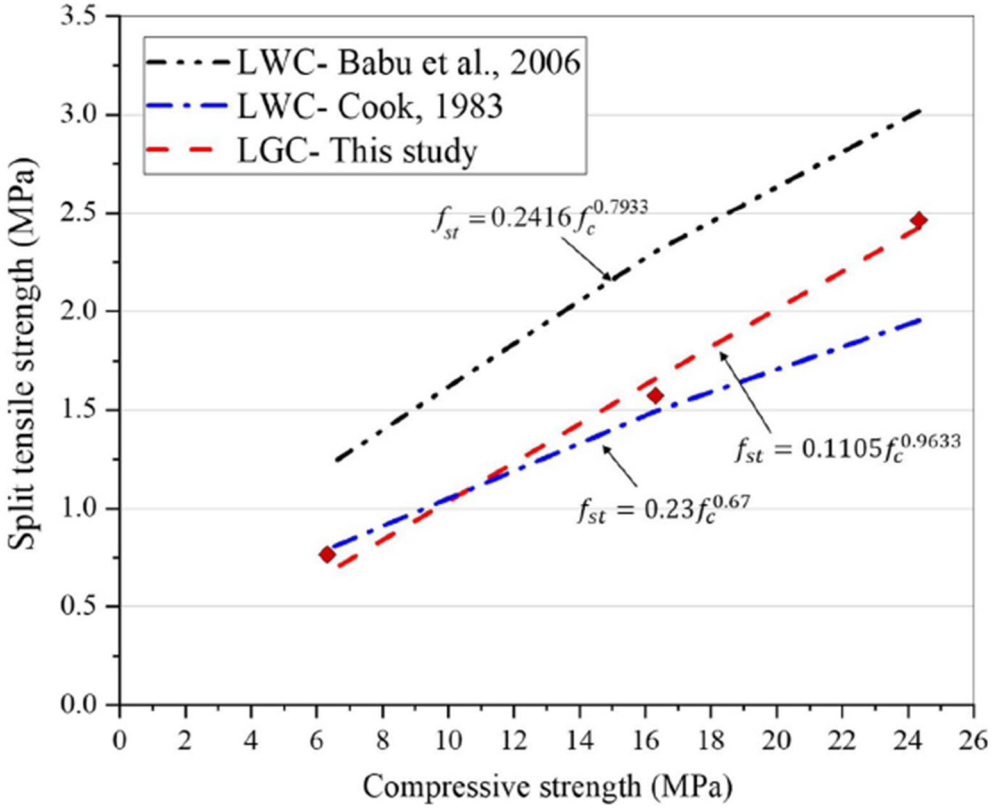

Fig. 13. Relationship between splitting tensile strength and compressive strength.

Fig. 13 shows the relationship between the splitting tensile strength and the compressive strength of LWC and LGC from the present study and previous studies. As observed, the decrease of EPS contents reduces the compressive strength of LGC, which results in the decrease of splitting tensile strength. This trend is consistent with the previous studies on LWC. Cook (1983) proposed an empirical model for the relationship between the splitting tensile strength and compressive strength of LWC, expressed as:

$$f_{st} = 0.23 f_c^{0.67} \tag{11}$$

where f_c is the compressive strength (MPa), f_{st} is the splitting tensile strength (MPa). As shown, the predicted value underestimates the splitting tensile strength of LGC when the compressive strength is higher than 10 MPa. Babu et al. (2006) also provided the following equation for predicting the splitting tensile strength of LWC containing EPS, which was made with different types of binder and EPS:

$$f_{st} = 0.2416 f_c^{0.7933} \tag{12}$$

It is shown that equation (12) overestimates the splitting tensile strength of LGC due to different types of binders and EPS beads were used in this study. Therefore, the proposed empirical model (R^2= 0.9712) based on the results from the present study for the relationship between the splitting tensile strength and compressive strength of the developed LGC with the density varying from 1284.31 to1791.86 kg/m^3 in this study is given by:

$$f_{st} = 0.1105 f_c^{0.9633} \tag{13}$$

Ultrasonic pulse velocity test

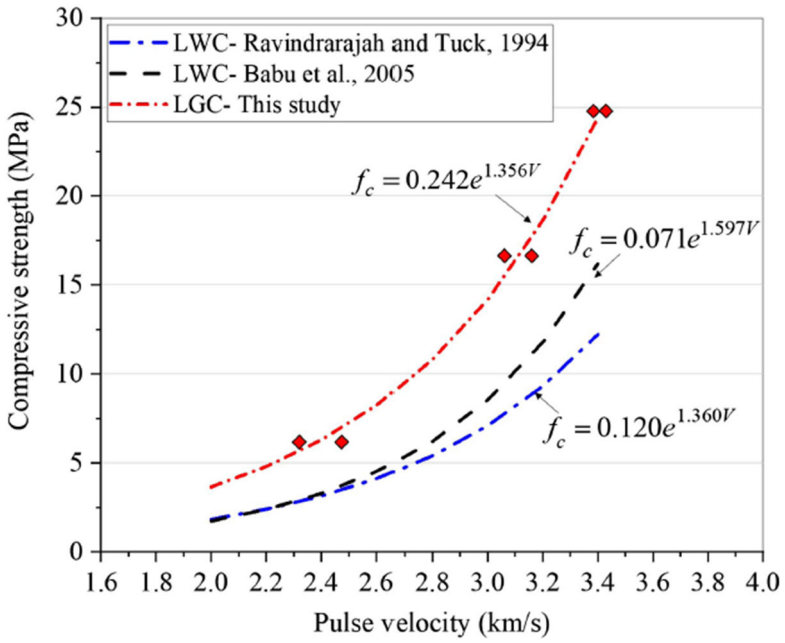

Fig. 14. Relationship between compressive strength and pulse velocity.

Table 3. Physical and mechanical properties of plain GM and LGC

Mix ID	ρ^a		f_c^a		E^a		μ^a		f_{st}^a		V^a
	(kg/m^3)	Std.	(MPa)	Std.	(GPa)	Std.	-	Std.	(MPa)	Std.	(km/s)
Plain GM	2204.41	28.4	61.12	1.43	16.74	0.71	0.10	0.02	5.21	0.19	4.29
EPS-10	1791.86	22.6	24.33	2.99	9.66	0.85	0.13	0.01	2.46	0.12	3.38
EPS-20	1634.67	94.2	16.31	1.98	7.38	0.23	0.15	0.04	1.47	0.33	3.06
EPS-30	1284.31	19.5	6.32	0.39	4.83	0.04	0.19	0.08	0.76	0.08	2.47

Note: Std. = standard deviation; ρ = density; f_c = compressive strength; E = modulus of elasticity; μ = Poisson's ratio; f_{st} = splitting tensile strength; V = ultrasonic pulse velocity.
[a]The result is 28-days mean value.

UPV test was carried out for the non-destructive evaluation of LGC strength and quality. Table 3 summarizes the mean values and standard deviations of the properties for all specimens tested in the present study. As shown, both compressive strength and UPV decrease as EPS content increases. Similar trends were observed in the previous study (Sadrmomtazi et al. 2012). Fig. 14 shows the relationship between the compressive strength and UPV from the present study and previous studies. As observed, the specimen with higher UPV has higher compressive strength. Ravindrarajah and Tuck (1994) proposed an empirical formula to predict the compressive strength of LWC made of chemical coated EPS from UPV, expressed as:

$$f_c = 0.120e^{1.360V} \tag{14}$$

where f_c is the compressive strength (MPa), and V is the pulse velocity (km/s). Babu et al. (2005) also proposed an empirical model for LWC with EPS:

$$f_c = 0.071e^{1.597V} \tag{15}$$

In general, it is found that the previous empirical formulae for LWC with EPS slightly underestimate the compressive strength of the developed LGC due to different types of binders and EPS beads were used in this study. In this regard, a new empirical formula (R^2= 0.9836) was proposed

to predict the compressive strength from UPV of the developed LGC with the density varying from 1284.31 to1791.86 kg/m^3 in this study as:

$$f_c = 0.242e^{1.356V} \quad (16)$$

XRD analysis

Fig. 15 (a) presents the XRD patterns of raw constituents of geopolymer. The amorphous sourced materials are presented by broad humps between the 2-theta angle at around 17° to 27° for FA and around 21° to 36° for slag. Several crystalline phases of Mullite (Al_6 Si_2O_{13}), Quartz (SiO_2), and Magnetite (Fe_3O_4) in the FA, and both Bassanite ($2CaSO_4 \cdot H_2O$) and Gypsum ($CaSO_4 \cdot 2H_2O$) in the slag are observed. As compared to raw material, the variations in both amorphous humps formation and crystalline peaks of Plain GM and LGC are evaluated by XRD analysis. Firstly, the comparison of the XRD pattern between Plain GM and LGC is shown in **Fig. 15** (b). The crystalline phases of Quartz (SiO_2), Mullite ($Al_6Si_2O_{13}$), Gypsum ($CaSO_4 \cdot 2H_2O$), and Sodalite ($Na_8(Al_6Si_6O_{24})Cl_2$) in both plain GM and LGC are detected. It is observed that the intensity of crystalline peaks of Quartz in LGC is lower than that in plain GM due to the substituting of fine aggregate with EPS in LGC.

Fig. 15 (c) presents a comparison of the XRD patterns between raw geopolymer constituents and plain GM. It is shown that some of the dominant peaks in the FA and slag disappear in plain GM and LGC. For instance, there is no sign of crystalline peaks at 2-theta angles of 11.68º, 14.77º, 25.71º, 29.74º, 31.91º for slag, and 35.62º, 37.51º, 54.13º for FA in XRD patterns of plain GM. This is attributed to Gypsum and Bassanite in slag and Magnetite in FA are dissolved to form amorphous geopolymer gel during the polymerization reaction. Furthermore, it is found that the crystalline peak at 2-theta angles of 16.45º in FA has much less intensity in regard to the plain GM. The same status

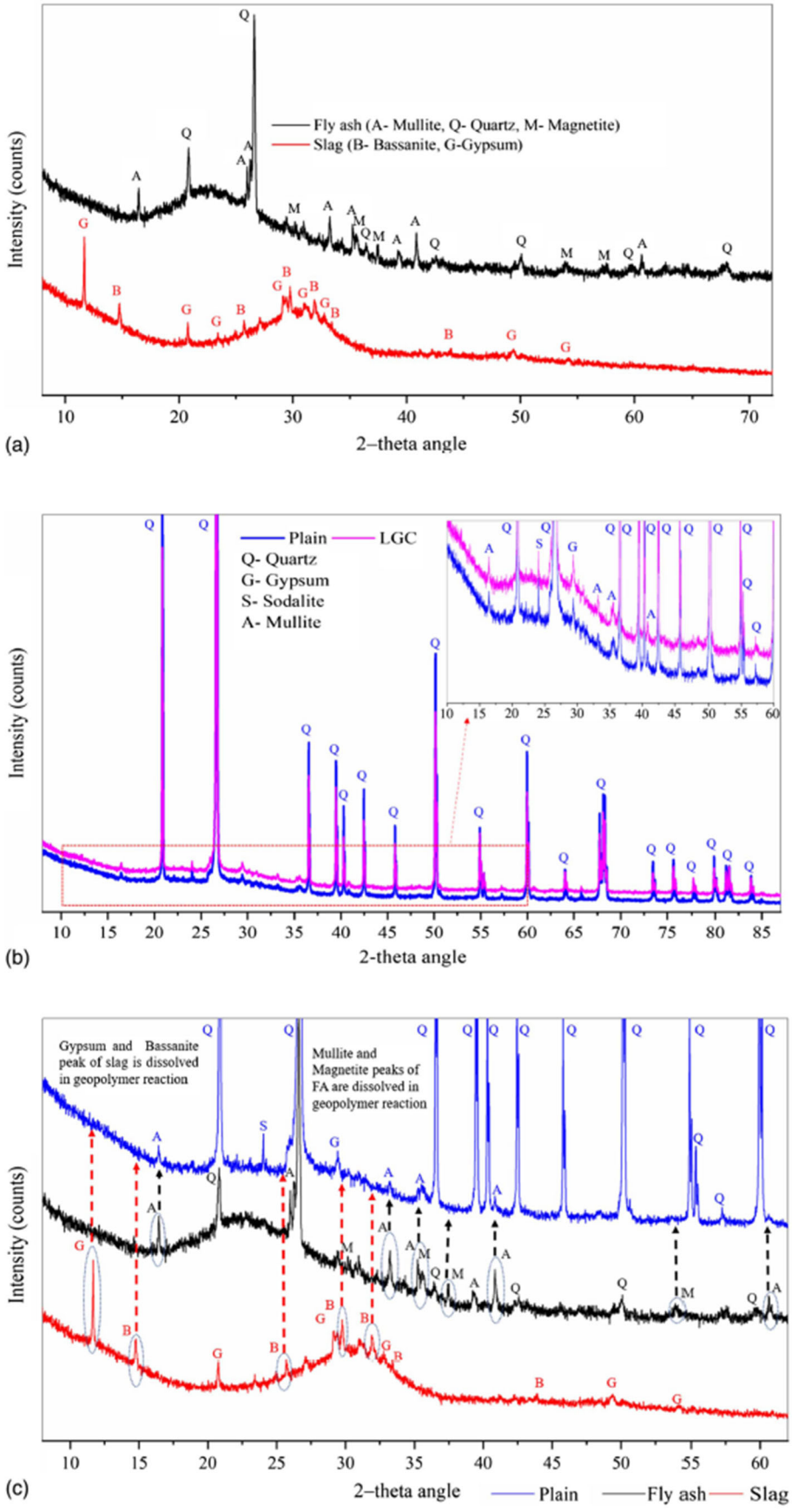

Fig. 15. XRD 2-theta (º) Cu, Kα patterns of (a) fly ash and slag; (b) plain GM and LGC; (c) comparison between raw ingredients and geopolymer.

can be observed at 2-theta angles of 33.23º, 35.23º, 40.85º and 60.64º, where the intensities of crystalline peaks of Mullite are lower than their original intensities in FA, which indicates that the majority of raw ingredients have reacted to form the geopolymer matrix. The XRD patterns of plain GM and raw ingredients are similar to the previous study on the high strength ambient-cured geopolymer composite (Khan et al. 2016).

SEM analysis

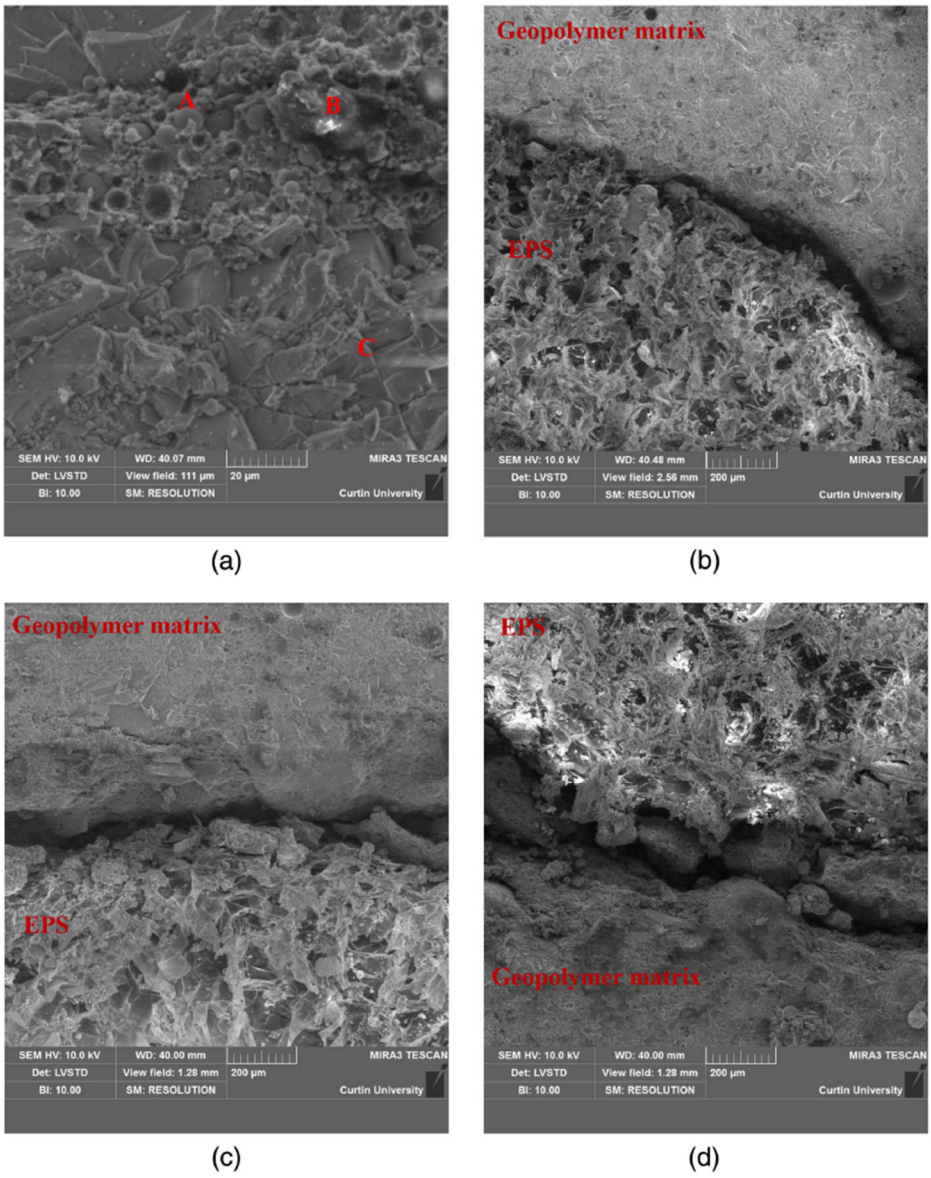

Fig. 16. SEM images of (a) plain GM and interface area between the geopolymer matrix and EPS; (b) EPS-10; (c) EPS-20; (d) EPS-30.

The microstructure of the plain GM specimen is shown in **Fig. 16**. Several partially reacted or unreacted FA particles indicated by symbol "A" can be seen in the SEM micrograph, and they are embedded within the geopolymer gel. Moreover, the structure of a dreierketten chain designated as symbol "B" results from the alkali activation of the FA-slag mix. This morphology is consistent with that typical observation for the poorly crystalline calcium silicate hydrate gel. Moreover, the typical homogeneous geopolymer gel marked as "C" is the main structural element of the geopolymer mortar. A similar microstructure of geopolymer mortar was also observed in the previous study (Khan et al. 2016). As observed, the compact and homogeneous geopolymer matrix is obtained at the microstructural level. **Fig. 16** (b), (c) and (d) present the SEM images of the ITZ between the EPS bead and the geopolymer matrix in LGC with different EPS content. It is observed that the ITZ becomes more distinct with an increase in EPS contents at a scale of 200 μm. It is because the strength of the matrix decreases as more natural fine aggregates are replaced by EPS, which results in the weak bonding. The weak bonding between EPS and matrix can reduce the compressive strength of LGC substantially when the volume fraction of EPS is 30% as reported in section Quasi-static compressive strength.

Conclusion

In this study, lightweight ambient-cured EPS geopolymer composites were developed by replacing natural fine aggregate with EPS beads at 10%, 20% and 30% in volume. The physical properties including density, workability, and ultrasonic pulse velocity of plain GM and LGC were evaluated. The mechanical properties such as compressive and splitting tensile strength, modulus of

elasticity and Poisson's ratio were obtained, followed by the XRD and SEM analysis. Based on the test results, the main conclusions can be drawn as follows:

1. The developed ambient-cured LGC achieved uniform distribution of EPS beads in the geopolymer matrix without evident segregation. It is worth noting that no admixture or bonding additive has been added in this study.
2. The plain GM with the designed mix proportion reached the compressive strength of 61.12 MPa at 28 days. The developed ambient-cured LGC (i.e. EPS-10, EPS-20, EPS-30) with the density of 1284.31~1791.86 kg/m^3 had the compressive strength of 6.32~24.33 MPa at 28 days. Among them, EPS-10 had the compressive strength of 24.33 MPa and density of 1791.86 kg/m^3, which met the requirements of structural lightweight concrete as specified in ACI 213R-14 (ACI 2014). Besides, EPS-20 obtained the compressive strength of 16.31 MPa and density of 1634.67 kg/m^3, which showed the properties of moderate strength lightweight concrete, therefore it could be used in non-structural applications, including but not limited to floors, panel walls, bricks, and blocks, etc.
3. The compressive strain capacity of plain GM was 0.36%. The reduction of compressive strain capacity of LGC was 33.33%, 41.66% and 63.89% by replacing natural aggregate with EPS beads in volume fractions of 10%, 20% and 30%, respectively, which indicates that the increase in EPS content could yield significant effects on the brittleness of LGC.
4. The EPS contents had significant effects on the physical and mechanical properties of the developed LGC. The density, workability, compressive strength, split tensile strength, modulus of elasticity decreased with the increase of EPS contents and the Poisson's ratio increased with the increase of EPS contents. The XRD results demonstrated well-reacted geopolymer matrix

and the substantial reduction in strength of EPS-30 can be interpreted by weak bonding between EPS and matrix as observed in the SEM analysis.

5. Empirical formulae were proposed to predict the compressive strength, modulus of elasticity, and splitting tensile strength of the developed LGC with various EPS contents.

Data Availability Statement

Some or all data, models, or codes that support the findings of this study are available from the corresponding author upon reasonable request.

Acknowledgements

The authors would like to thank the financial support from the Australian Research Council via Laureate Fellowship FL180100196.

Reference

ACI (2014). *Guide for Structural Lightweight Aggregate Concrete*, ACI 213R-14, . Farmington Hills, MI.

Amianti, M., and Botaro, V. R. (2008). "Recycling of EPS: A new methodology for production of concrete impregnated with polystyrene (CIP)." *Cement and Concrete Composites*, 30(1), 23-28.

Aslam, M., Shafigh, P., Jumaat, M. Z., and Lachemi, M. (2016). "Benefits of using blended waste coarse lightweight aggregates in structural lightweight aggregate concrete." *Journal of Cleaner Production*, 119, 108-117.

Aslani, F., Deghani, A., and Asif, Z. (2020). "Development of Lightweight Rubberized Geopolymer Concrete by Using Polystyrene and Recycled Crumb-Rubber Aggregates." *Journal of Materials in Civil Engineering*, 32(2), 04019345.

ASTM (2014). "Standard Test Method for Density and Void Content of Freshly Mixed Pervious Concrete." *ASTM C1688-14*.

ASTM (2014). "Standard Test Method for Static Modulus of Elasticity and Poisson's Ratio of Concrete in Compression." *ASTM C469-14*.

ASTM (2015). "Standard Test Method for Flow of Hydraulic Cement Mortar." *ASTM C1437-15*.

ASTM (2016). "Standard Guide for Examination of Hardened Concrete Using Scanning Electron Microscopy." *ASTM C1723-16*.

ASTM (2016). "Standard Test Method for Pulse Velocity Through Concrete." *ASTM C597-16*.

ASTM (2017). *Standard Test Method for Splitting Tensile Strength of Cylindrical Concrete Specimens*, ASTM C496-17. West Conshohocken, PA.

ASTM (2018). "Standard Test Method for Compressive Strength of Cylindrical Concrete Specimens." *ASTM C39-18*.

ASTM (2019). "Standard Specification for Coal Fly Ash and Raw or Calcined Natural Pozzolan for Use in Concrete." *ASTM C618-19*.

Atiş, C., Görür, E., Karahan, O., Bilim, C., İlkentapar, S., and Luga, E. (2015). "Very high strength (120 MPa) class F fly ash geopolymer mortar activated at different NaOH amount, heat curing temperature and heat curing duration." *Construction and Building Materials*, 96, 673-678.

Babu, D. S., Babu, K. G., and Tiong-Huan, W. (2006). "Effect of polystyrene aggregate size on strength and moisture migration characteristics of lightweight concrete." *Cement and Concrete Composites*, 28(6), 520-527.

Babu, D. S., Babu, K. G., and Wee, T. (2005). "Properties of lightweight expanded polystyrene aggregate concretes containing fly ash." *Cement and Concrete Research*, 35(6), 1218-1223.

Babu, K. G., and Babu, D. S. (2003). "Behaviour of lightweight expanded polystyrene concrete containing silica fume." *Cement and Concrete Research*, 33(5), 755-762.

Benhelal, E., Zahedi, G., Shamsaei, E., and Bahadori, A. (2013). "Global strategies and potentials to curb CO2 emissions in cement industry." *Journal of cleaner production*, 51, 142-161.

Bogas, J. A., de Brito, J., and Figueiredo, J. M. (2015). "Mechanical characterization of concrete produced with recycled lightweight expanded clay aggregate concrete." *Journal of Cleaner Production*, 89, 187-195.

Chuah, S., Duan, W., Pan, Z., Hunter, E., Korayem, A. H., Zhao, X. L., Collins, F., and Sanjayan, J. G. (2016). "The properties of fly ash based geopolymer mortars made with dune sand." *Materials & Design*, 92, 571-578.

Colangelo, F., Roviello, G., Ricciotti, L., Ferrandiz-Mas, V., Messina, F., Ferone, C., Tarallo, O., Cioffi, R., and Cheeseman, C. (2018). "Mechanical and thermal properties of lightweight geopolymer composites." *Cement and Concrete Composites*, 86, 266-272.

Cook, C. (1983). "FIP manual of lightweight aggregate concrete: Published by The Surrey University Press, Bishopriggs, Glasgow G64 2NZ, Scotland, 1983 ISBN 0 903384 43 4, 259 pp." Elsevier.

Demirel, B. (2013). "Optimization of the composite brick composed of expanded polystyrene and pumice blocks." *Construction and Building Materials*, 40, 306-313.

Doroudiani, S., and Omidian, H. (2010). "Environmental, health and safety concerns of decorative mouldings made of expanded polystyrene in buildings." *Building and Environment*, 45(3), 647-654.

Falzone, G., Falla, G. P., Wei, Z., Zhao, M., Kumar, A., Bauchy, M., Neithalath, N., Pilon, L., and Sant, G. (2016). "The influences of soft and stiff inclusions on the mechanical properties of cementitious composites." *Cement and Concrete Composites*, 71, 153-165.

Feng, K. N., Ruan, D., Pan, Z., Collins, F., Bai, Y., Wang, C. M., and Duan, W. H. (2014). "Effect of strain rate on splitting tensile strength of geopolymer concrete." *Magazine of Concrete Research*, 66(16), 825-835.

Ferrándiz-Mas, V., and García-Alcocel, E. (2013). "Durability of expanded polystyrene mortars." *Construction and Building Materials*, 46, 175-182.

Glenn, G., Miller, R., and Orts, W. (1998). "Moderate strength lightweight concrete from organic aquagel mixtures." *Industrial Crops and Products*, 8(2), 123-132.

Hansen, T. C., and Nielsen, K. E. "Influence of aggregate properties on concrete shrinkage." *Proc., Journal Proceedings*, 783-794.

Hobbs, D. (1969). "Bulk modulus shrinkage and thermal expansion of a two phase material." *Nature*, 222(5196), 849-851.

Hobbs, D. "Influence of aggregate restraint on the shrinkage of concrete." *Proc., Journal Proceedings*, 445-450.

Hu, Y., Tang, Z., Li, W., Li, Y., and Tam, V. W. (2019). "Physical-mechanical properties of fly ash/GGBFS geopolymer composites with recycled aggregates." *Construction and Building Materials*, 226, 139-151.

Huntzinger, D. N., and Eatmon, T. D. (2009). "A life-cycle assessment of Portland cement manufacturing: comparing the traditional process with alternative technologies." *Journal of Cleaner Production*, 17(7), 668-675.

Kakali, G., Kioupis, D., Skaropoulou, A., and Tsivilis, S. "Lightweight geopolymer composites as structural elements with improved insulation capacity." *Proc., MATEC Web of Conferences*, EDP Sciences.

Kan, A., and Demirboğa, R. (2009). "A novel material for lightweight concrete production." *Cement and Concrete Composites*, 31(7), 489-495.

Khan, M. Z. N., Hao, Y., and Hao, H. (2016). "Synthesis of high strength ambient cured geopolymer composite by using low calcium fly ash." *Construction and Building Materials*, 125, 809-820.

Khandelwal, M., Ranjith, P., Pan, Z., and Sanjayan, J. G. (2013). "Effect of strain rate on strength properties of low-calcium fly-ash-based geopolymer mortar under dry condition." *Arabian Journal of Geosciences*, 6(7), 2383-2389.

Leemann, A., Lura, P., and Loser, R. (2011). "Shrinkage and creep of SCC–The influence of paste volume and binder composition." *Construction and Building Materials*, 25(5), 2283-2289.

Liu, N., and Chen, B. (2014). "Experimental study of the influence of EPS particle size on the mechanical properties of EPS lightweight concrete." *Construction and Building Materials*, 68, 227-232.

Miled, K., Sab, K., and Le Roy, R. (2007). "Particle size effect on EPS lightweight concrete compressive strength: Experimental investigation and modelling." *Mechanics of Materials*, 39(3), 222-240.

Nasvi, M., Rathnaweera, T., and Padmanabhan, E. (2016). "Geopolymer as well cement and its mechanical integrity under deep down-hole stress conditions: application for carbon capture and storage wells." *Geomechanics and Geophysics for Geo-Energy and Geo-Resources*, 2(4), 245-256.

Nath, P., and Sarker, P. K. (2014). "Effect of GGBFS on setting, workability and early strength properties of fly ash geopolymer concrete cured in ambient condition." *Construction and Building Materials*, 66, 163-171.

Pan, Z., and Sanjayan, J. G. (2010). "Stress–strain behaviour and abrupt loss of stiffness of geopolymer at elevated temperatures." *Cement and Concrete Composites*, 32(9), 657-664.

Pan, Z., Sanjayan, J. G., and Rangan, B. V. (2011). "Fracture properties of geopolymer paste and concrete." *Magazine of Concrete Research*, 63(10), 763-771.

Pauw, A. (1960). *Static modulus of elasticity of concrete as affected by density*, University of Missouri.

Pelisser, F., Barcelos, A., Santos, D., Peterson, M., and Bernardin, A. M. (2012). "Lightweight concrete production with low Portland cement consumption." *Journal of Cleaner Production*, 23(1), 68-74.

Perry, S., Bischoff, P., and Yamura, K. (1991). "Mix details and material behaviour of polystyrene aggregate concrete." *Magazine of Concrete Research*, 43(154), 71-76.

Posi, P., Ridtirud, C., Ekvong, C., Chammanee, D., Janthowong, K., and Chindaprasirt, P. (2015). "Properties of lightweight high calcium fly ash geopolymer concretes containing recycled packaging foam." *Construction and Building Materials*, 94, 408-413.

Provis, J. L., and Van Deventer, J. S. J. (2009). *Geopolymers: structures, processing, properties and industrial applications*, Elsevier.

Ravindrarajah, R. S., and Tuck, A. (1994). "Properties of hardened concrete containing treated expanded polystyrene beads." *Cement and Concrete Composites*, 16(4), 273-277.

Sadrmomtazi, A., Sobhani, J., Mirgozar, M. A., and Najimi, M. (2012). "Properties of multi-strength grade EPS concrete containing silica fume and rice husk ash." *Construction and Building Materials*, 35, 211-219.

Shin, C. (2006). "Filtration application from recycled expanded polystyrene." *Journal of Colloid and Interface Science*, 302(1), 267-271.

Singh, B., Ishwarya, G., Gupta, M., and Bhattacharyya, S. (2015). "Geopolymer concrete: A review of some recent developments." *Construction and Building Materials*, 85, 78-90.

Tamut, T., Prabhu, R., Venkataramana, K., and Yaragal, S. C. (2014). "Partial replacement of coarse aggregates by expanded polystyrene beads in concrete." *International Journal of Research in Engineering and Technology*, 3(02), 238-241.

Tang, W., Balendran, R., Nadeem, A., and Leung, H. Y. (2006). "Flexural strengthening of reinforced lightweight polystyrene aggregate concrete beams with near-surface mounted GFRP bars." *Building and Environment*, 41(10), 1381-1393.

Tang, W., Cui, H., and Tahmasbi, S. (2016). "Fracture properties of polystyrene aggregate concrete after exposure to high temperatures." *Materials*, 9(8), 630.

Tang, W., Cui, H., and Wu, M. (2014). "Creep and creep recovery properties of polystyrene aggregate concrete." *Construction and Building Materials*, 51, 338-343.

Tang, W., Lo, Y., and Nadeem, A. (2008). "Mechanical and drying shrinkage properties of structural-graded polystyrene aggregate concrete." *Cement and Concrete Composites*, 30(5), 403-409.

Tang, Z., Li, W., Tam, V. W., and Luo, Z. (2020). "Investigation on dynamic mechanical properties of fly ash/slag-based geopolymeric recycled aggregate concrete." *Composites Part B: Engineering*, 185, 107776.

Tao, Z., and Pan, Z. (2019). "Geopolymer concrete at ambient and elevated temperatures: recent developments and challenges." *NED University Journal of Research*, 2, 113-127.

Topçu, I. B. (1997). "Semi lightweight concretes produced by volcanic slags." *Cement and Concrete Research*, 27(1), 15-21.

Xu, Y., Jiang, L., Xu, J., and Li, Y. (2012). "Mechanical properties of expanded polystyrene lightweight aggregate concrete and brick." *Construction and Building Materials*, 27(1), 32-38.

Yoo, T. K., and Qiu, T. (2018). "Optimization of constitutive model parameters for simulation of polystyrene concrete subjected to impact." *International Journal of Protective Structures*, 9(2), 121-140.